Gyrokinetic-ion drift-kinetic-electron simulation of the (m = 2, n = 1) cylindrical tearing mode

Y. Chen, J. Chowdhury, N. Maksimovic, S. E. Parker, and W. Wan

Citation: Physics of Plasmas **23**, 056101 (2016); doi: 10.1063/1.4943105
View online: https://doi.org/10.1063/1.4943105
View Table of Contents: http://aip.scitation.org/toc/php/23/5
Published by the American Institute of Physics

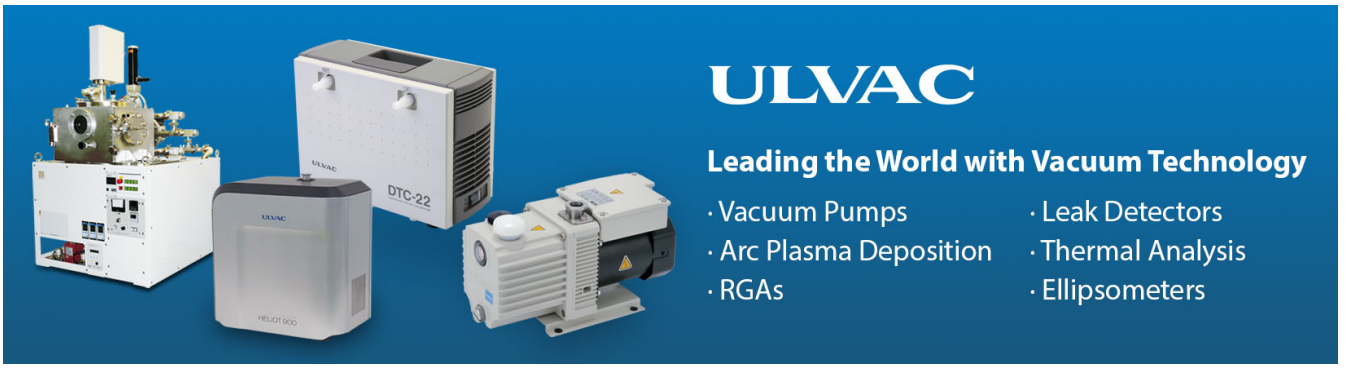

Gyrokinetic-ion drift-kinetic-electron simulation of the (m = 2, n = 1) cylindrical tearing mode

Y. Chen,[a] J. Chowdhury, N. Maksimovic, S. E. Parker, and W. Wan
University of Colorado at Boulder, Boulder, Colorado 80309, USA

(Received 19 November 2015; accepted 7 December 2015; published online 4 March 2016)

Particle-in-cell simulations of $(m = 2, n = 1)$ tearing mode in cylindrical plasmas are carried out with kinetic electrons using the split-weight control-variate algorithm [Y. Chen and S. E. Parker, J. Comput. Phys. **220**, 839 (2007)]. Radially, global simulation shows global mode structure in agreement with reduced-magnetohydrodynamic eigenmode calculation. Simulations of the tearing layer are verified with analytic results for the collisionless, semi-collisional, and drift-tearing mode. [http://dx.doi.org/10.1063/1.4943105]

I. INTRODUCTION

Electron kinetic effects are essential for an accurate description of the tearing mode in present day tokamak plasmas. In such plasmas, the high electron temperature leads to a low electron collision rate, which makes any fluid model, such as resistive magnetohydrodynamics (MHD), a poor approximation for the tearing layer. Even if a closure scheme based on linear kinetic theory is used in the fluid model, as is done in gyrofluid theory, the validity of such a model for the nonlinear evolution of the tearing mode is not guaranteed and is to be verified with a kinetic model. At the present time, the most promising approach to modeling the neoclassical tearing mode (NTM) is a hybrid approach, in which the macroscopic quantities, e.g., the quasi-steady magnetic equilibrium and the density/temperature profiles, are evolved using fluid models, and the plasma current is obtained with a kinetic model. This is a multiple-time-scale approach, where it is assumed that the macroscopic time scale for the island growth is well separated from the microscopic time scale of ion and electron kinetic response to the magnetic equilibrium and the formation of electric current. The kinetic problem in such a multiple-scale approach is that of computing the neoclassical current and transport coefficients in a three-dimensional (3D) magnetic field, which comes from magnetohydrodynamic simulations. The neoclassical current can then be used in the MHD simulation to evolve the magnetic configuration. An axisymmetric version of such an integrated modeling has been attempted by Lyons *et al.*[1] This multiple-scale approach is, however, not valid for the initial growth of the seeding island, as at the initial stage, the island size is small (less than the ion Larmor radius), and kinetic effects are essential for the island dynamics. In the linear and early nonlinear phase of the mode, a direct kinetic model is therefore needed.

In this paper, we extend the gyrokinetic particle-in-cell (PIC) code GEM, initially developed for drift-wave turbulence simulations, to the $n = 1$ tearing mode. Part of this extension has been recently reported for the gyrokinetic ion/mass-less fluid electron model,[2] where new field solvers and discretization schemes are developed that avoid the usual high-n approximations when using the field-aligned coordinates. The same extension has now been carried over to the fully drift-kinetic electron model of GEM that is based on the split-weight control-variate algorithm.[3,4] Although gyrokinetic simulations with kinetic electrons have been used to study tearing modes by many authors,[5–11] most of the studies are for small scale tearing modes such as the micro-tearing modes. Low-n tearing modes in present day tokamaks pose a special challenge to simulations with kinetic electrons, as high resolution is needed to resolve the thin tearing layer and long time simulations are needed due to the small mode growth rate. In addition to these requirements mandated by physical mode characteristics, modes with small perpendicular wavenumber $k_\perp \rho_i$ (ρ_i is the ion Larmor radius) also incur numerical difficulties (constraint on the time step and accuracy problems) that are particularly challenging to the PIC method. Verification of a kinetic electron algorithm for drift waves (including the ∇T_e-driven micro-tearing modes) does not warrant its applicability for low-n tearing modes, as the severity of numerical problems changes with wavenumber. Our first goal is to verify GEM's kinetic electron algorithm for low-n tearing modes, specifically tearing modes in the collisionless and semi-collisional regime,[12] where kinetic effects are known to be important and analytic scaling laws are available for simulation/theory comparison. It turns out quite challenging to use analytic scaling laws for verification, as one needs to ensure that the validity criteria for the scaling behaviour be fulfilled. For instance, the semi-collisional scaling of $\gamma \sim \nu^{1/3}$ (γ is the growth rate and ν is the collision rate) is not observed in a recent study with the Eulerian code GKW;[10] instead a much weaker scaling, $\gamma \sim \nu^{1/7}$, is seen. This disagreement can be understood by checking the mode characteristics with the assumptions used to derive the scaling laws; in some cases, one can show that the constant-Ψ approximation[13] is not valid. The global feature of the mode (the external solution that is to be matched to the tearing layer solution), on the other hand, is largely determined by the MHD model and does not involve kinetic electron effects. Ideally, we would like to carry out simulations in the full radial domain and verify the simulation with both the global

Note: Paper PI3 5, Bull. Am. Phys. Soc. **60**, 262 (2015).
[a]Invited speaker.

mode structure and the analytic scaling laws; this would provide a very strong verification of the code. But such simulation is found to be impractical with the present code using uniformly spaced radial grids. This difficulty is overcome by using a radial domain much smaller than the minor radius, with an imposed boundary condition that generalizes the tearing mode parameter Δ'.[2] Using a reduced radial size allows us to fully resolve the tearing layer and choose equilibrium parameters that satisfy the criteria for the analytic scaling results. We are now able to observe the correct scaling behaviors in both the collisionless regime and the semi-collisional regime. All simulations in this paper are linear, and a cylindrical equilibrium is used to facilitate direct comparison with analytic theory. Nonlinear simulations and toroidal effects will be presented in a forthcoming paper.

This paper is organized as follows. In Section II, we test the GEM algorithm for the long wavelength shear Alfven waves in a 3D slab and summarize our previous findings on how to include kinetic electrons in gyrokinetic simulations. Tearing mode simulations are presented in Section III, and summary is given in Section IV.

II. COMMENTS ON KINETIC ELECTRON ALGORITHMS

The small electron mass incurs a constraint on the time step (vaguely termed as "the Courant condition") and an accuracy problem (called the "Cancellation Problem"[3,14]). The accuracy problem occurs only in simulations with magnetic field perturbations, as in shear Alfven waves and tearing modes. Our first task is to test the split-weight control-variate algorithm[3] for shear Alfven waves in the long wavelength limit. For convenience, we briefly summarize the GEM algorithm as follows. The field is represented by the electric potential ϕ and the parallel component of the vector potential, $A_\parallel$, obtained from the quasi-neutrality condition and the parallel Ampere's equation, respectively. The parallel canonical momentum $p_\parallel = v_\parallel + (q/m)A_\parallel$ is used as the parallel velocity coordinate. The electron distribution is split as $f_e = f_0(p_\parallel) + \epsilon(e\phi/T_e)f_0 + h$ (T_e is the equilibrium electron temperature), and h is directly represented by the electron weights. The split-weight parameter is usually chosen to be $\epsilon = 1$ in this paper. The explicit appearance of ϕ in f_e leads to an additional field equation for $\dot{\phi} \equiv \partial\phi/\partial t$, derived from the quasi-neutrality condition and called as the vorticity equation. Using $p_\parallel$ as the velocity coordinate leads to a stiff form of the Ampere's equation, which is solved with the control-variate method.[3,15] This scheme is initially developed in a flux-tube, later extended to general geometry. It has been extensively benchmarked with Eulerian codes for high-n drift waves, such as the ion-temperature-gradient-driven modes (ITG) and the trapped electron modes.[16] Here, as a first step toward applying the algorithm to the $n = 1$ tearing mode, we test it for the long wavelength shear Alfven waves in a shearless 3D slab. The mode has a wavenumber $k_\perp\rho_u = 0.01$ and $k_\parallel\rho_u = 0.000714$. Here $\rho_u = m_p v_u/eB$ is the proton Larmor radius in the uniform magnetic field with magnitude B and at a reference temperature $T_u = m_p v_u^2$, in this paper taken to be the electron temperature at the mode location. The corresponding Larmor frequency $\omega_u = eB/m_p$ is used to normalize frequency and time. Drift waves typically have $k_\perp\rho_u > 0.1$, and $k_\perp\rho_u = 0.01$ roughly corresponds to the $m = 2$ mode in a DIII-D[17] plasma. The numerical difficulty with kinetic electrons scales as $\sim 1/k_\perp^2$.

Fig. 1 shows the simulated shear Alfven wave frequency in comparison with the shear Alfven dispersion relation. They agree very well for beta values up to $\beta = 25\%$. Here, $\beta = 2(n_i T_i + n_e T_e)/\mu_0 B^2$, and $T_i = T_e$ is the ion and electron temperature, $n_i = n_e$ is the density. The time step is $\omega_u \Delta t = 0.5$. The mode propagates in the $y - z$ plane and the number of spatial grids is $(N_x, N_y, N_\parallel) = (4, 128, 128)$, with 512 particles per cell per species. Resolution in both the velocity space (measured by the number of particles per spatial cell) and the real space is unusually high for a single wave simulation, as one expects a spatial resolution of ~ 16 per wavelength to give an accurate description of the wave. The fine resolution is necessary as a consequence of the low wavenumber; a grid number of $N_y = 32$ leads to a frequency nearly double the dispersion relation result for the $\beta = 0.25$ case. The fields $A_\parallel/\phi$ are filtered after each field solving so that only the wave of interest is retained, and no grid-scale modes are possible, yet the small time step is needed for numerical stability, despite the use of the split-weight scheme. Without the split-weight scheme, i.e., setting $\epsilon = 0$, the simulation appears to be unconditionally unstable at high β values. These observations reveal the challenging aspects of gyrokinetic simulations applied to long wavelength modes. Much recent progress has been made in this area by Mishchenko *et al.*,[15] whose mixed-variable algorithm[15] appears to be an alternative to the split-weight scheme for achieving numerical stability.

Both Mishchenko's mixed-variable algorithm and the GEM algorithm can be viewed as direct methods for the gyrokinetic Maxwell system of equations. These algorithms are direct in the sense that the quasi-neutrality condition and the Ampere's equation are directly solved for ϕ and $A_\parallel$, respectively. We have also explored an alternative scheme based on closing a fluid-electron model with kinetic particles (the "closure" scheme).[16,18] The closure scheme is not direct

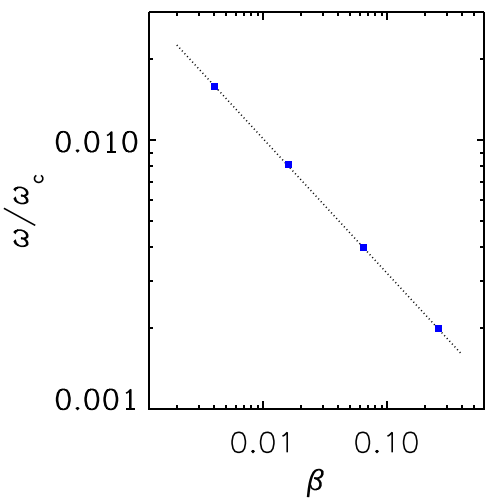

FIG. 1. Shear Alfven wave frequency vs. beta, $k_\perp\rho_u = 0.01$. Points are simulation results, dashed line for dispersion relation. $\omega_c = \omega_u$ is the proton cyclotron frequency.

in that the vorticity equation is used instead of the quasi-neutrality condition, and the Ampere's equation is solved "backwards" to obtain the electron flow from a known $A_\parallel$. In principle, the closure scheme can be exact, i.e., the electron pressure terms in the fluid equations are calculated from the particle distribution without approximations; in this case, the closure scheme and the direct methods are mathematically equivalent. We have considered the closure scheme for the present study, but now prefer the direct method. The reason is that for tearing modes, accurate calculation of the parallel electric field in the tearing layer is crucial; therefore, an intrinsic difficulty due to the fast electron parallel motion is unavoidable. When the accuracy problem is present, solving it in the direct method is much easier than solving it in a non-direct method. It is useful to summarize our current understanding of these alternate algorithms as follows:

(1) If kinetic electron effects are to be calculated exactly, then a cancellation problem cannot be avoided. It is easier to solve this problem in the Ampere's equation than in the generalized Ohm's law;
(2) In simple geometry, the cancellation problem can be solved by replacing the field equation with the form with finite grid-size corrections in the large particle number limit.[19] In general, the problem is best solved with the control-variate method, as in addition to finite-grid-size errors, there might be a systematic deviation between the actual marker distribution and the assumed equilibrium distribution in a complex geometry, where particle trapping/drift is important. Systematic error due to this effect will be cancelled with the control-variate method;
(3) The split-weight scheme is mainly a technique for numerical stability and can be replaced by other methods such as the mixed-variable approach;
(4) For some kinetic-MHD phenomena such as the energetic-particle-driven Alfven eigenmodes, an accurate calculation of the parallel electric field is not essential. In this case, the closure scheme with an approximate kinetic closure, or even a fluid electron model, can be used for better computational efficiency.

III. CYLINDRICAL (2, 1) TEARING MODE SIMULATIONS

We consider a cylindrical equilibrium with the safety factor profile $q(r) = 1.5(1 + (r/a)^2)$ and a constant density. The plasma has a single hydrogen ion species. The on-axis plasma beta is $\beta(0) = 0.004$. The aspect ratio is fixed at $R_0/a = 4$, but the size is varied from $a = 50\rho_u$ to $a = 370\rho_u$. The q-profile and the self-consistent equilibrium electron flow profile are the same as in the previous work,[2] where the extension of the fluid electron model to low-n is described in detail. The extension of the direct method to low-n is similar. The equilibrium parallel electron flow is modeled by a driving term in the electron weight equation. Electrons are loaded according to the unshifted Maxwellian, regardless of the magnitude of the equilibrium flow. The field variables $A_\parallel/\phi$ are decomposed poloidally and toroidally, and, in the radial direction, discretized pseudo-spectrally in the case of quasi-neutrality condition, and with the finite-difference method in the case of Ampere's equation. A mapping between the toroidal coordinates and the field-aligned coordinates is explicitly constructed to facilitate the transformation in coordinates between particle pushing and field solving. In the cylindrical equilibrium, there is no poloidal coupling. We study the $(m, n) = (2, -1)$ tearing mode, which has a tearing layer located near the $q = 2$ surface at $r/a = 0.577$. Our main goal is to verify the simulation for the collisionless and semi-collisional tearing mode, for which the kinetic electron effects are crucial and the ions are neither physically important nor causing any computational problem. In the following simulations, we frequently neglect ion dynamics other than the polarization effect, as is also done in the theoretical analysis.[12]

Analytical results used for comparison include the collisionless tearing mode growth rate

$$\gamma_k = k_y v_e (\Delta' a)/2k_0^2 a l_s \sqrt{\pi}, \tag{1}$$

the collisionless characteristic length of the tearing layer

$$\Delta_k = (\Delta' a)/2\sqrt{\pi} k_0^2 a, \tag{2}$$

the semi-collisional tearing mode growth rate

$$\gamma_{sc} = \left(\frac{3\pi^{1/4}}{4\Gamma(11/4)}\right)^{2/3} \gamma_k^{2/3} \nu_c^{1/3}, \tag{3}$$

the semi-collisional characteristic length of the tearing layer

$$\Delta_{sc} = \left(\frac{\nu_c}{\gamma_k}\right)^{2/3} \Delta_k, \tag{4}$$

the collisionless drift-tearing mode real frequency

$$\omega_1 = \omega_n^* + \omega_T^*/2, \tag{5}$$

and the characteristic length of the collisionless drift-tearing mode,

$$\Delta = \left(1 + \frac{\omega_1^{*2}}{\gamma_k^2}\right)^{1/2} \Delta_k. \tag{6}$$

These results are taken from Drake and Lee.[12] Here, $k_y = m/r_s$ is the mode wavenumber at the resonance location $r = r_s$, $k_0 = \omega_{pe}/c$, ω_{pe} is the electron plasma frequency, c is the light speed; the thermal speed is defined as $v_e = \sqrt{2T_e/m_e}$, m_e is the electron mass; the magnetic shear length is $l_s = R_0 q_0^2/rq'$ at the tearing layer; ν_c is the electron collision frequency; $\omega_n^* = k_y T_e/eB|\nabla n_e/n_e|$ and $\omega_T^* = k_y T_e/eB|\nabla T_e/T_e|$; and the tearing mode parameter Δ' is defined to be the jump of $A_\parallel'(r)$ across the tearing layer. We do not attempt to verify simulations for the collisional regime, because it is difficult to find cases where the validity condition for the collisional regime is satisfied, and numerically a large collision rate requires small time steps and a large number of particles to reduce noise. Tearing modes in present day tokamaks are in the semi-collisional regime.[12]

The difficulty in simulating a global tearing mode can be appreciated by estimates based on these formulas. For a

tokamak with $a = 200\rho_u$, $\beta = 0.004$, and $\Delta' a = 6$, the $m = 2$ mode has a collisionless growth rate of $\gamma_k/\omega_u = 1.5 \times 10^{-6}$ and a tearing layer width of $\Delta_k/\rho_u = 0.0046$. The growth rate is about 100 times smaller than typical drift wave growth rate, and the tearing layer width is much smaller than the electron Larmor radius ($\sim\rho_i/50$). At this scale, the drift-kinetic electron model used in theoretical analysis is not valid, and the electrons must be treated with gyrokinetics. This observation is relevant for most of the cases studied here, including the semi-collisional tearing modes and the drift-tearing modes where the tearing layer width is significantly broadened. This observation, however, does not affect the comparison between simulation and analytic results, as the drift-kinetic electron model is also used in the simulations. It is also clear that for most plasmas of interest, it is impractical to simulate the entire plasma cross-section. Assume that 10 radial grid points are needed to resolve the tearing layer, the total number of radial grids would be 4×10^5! Including collisions and ω^* effect will greatly reduce the number of radial grids, but for a DIII-D sized plasma, the computational requirement is still prohibitive. In the following simulations, a much reduced radial domain will be used, with the radial boundary conditions for $A_\parallel$ obtained from global reduced-MHD eigenmode calculations.[2] Nevertheless, it is important to carry out a global simulation, even if only for a small size plasma, with reasonable radial resolution, and compare the global mode structure with the eigenmode result to ensure that the global mode structure is adequately captured with the kinetic electron algorithm.

The global mode structure from simulation is shown in Fig. 2, for a plasma with $a = 50\rho_u$. This is a case of pure tearing mode with $\omega* = 0$, and a collision rate of $\nu_c/\omega_u = 1.04 \times 10^{-4}$. The semi-collisional tearing layer width is calculated to be $\Delta_{sc}/\rho_u = 0.065$. The tearing mode parameter is taken to be $\Delta' a = 6$. The time step is $\omega_u \Delta t = 5$, the radial

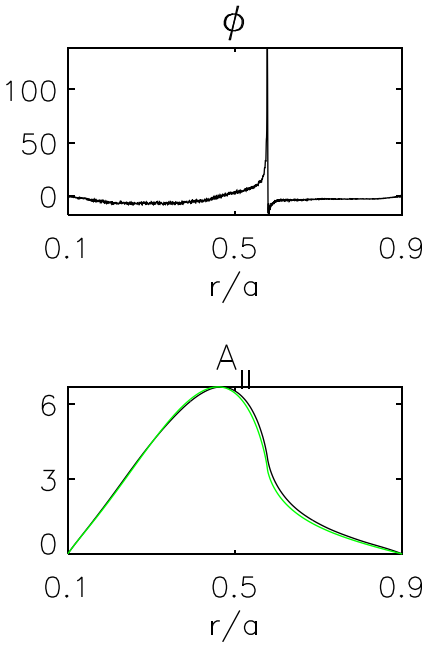

FIG. 2. Top: radial mode structure for ϕ. Bottom: radial mode structure for $A_\parallel$, the green line is from reduced-MHD eigenmode calculation. The minor radius is $a = 50\rho_u$, the number of radial grid points is $N_x = 2048$.

domain is $0.1 < r/a < 0.9$ with the number of grids $(N_x, N_y, N_\parallel) = (2048, 64, 64)$ in each dimension, so that $\Delta_{sc}/\Delta x \approx 3$. The number of particles is 8/cell. The simulation yields a mode growth rate of $\gamma/\omega_u = 1.9 \times 10^{-4}$, compared with the theoretical semi-collisional growth rate of $\gamma_{sc} \approx 1 \times 10^{-4}$. As will soon to be shown, this case is not in the asymptotic regime even for the collisionless tearing mode where the tearing layer width is much smaller (hence, asymptotic analysis is more likely to be valid). The global mode structure from the simulation agrees well with the eigenmode result. This is expected, as both the eigenmode analysis and the simulation use the same cylindrical equilibrium, and the reduced-MHD model is a good approximation to the kinetic model in the external region. One might conjecture that the global mode structure is insensitive to the numerical resolution in the tearing layer, and the same global mode structure will emerge with reduced radial resolution as long as the mode is unstable, although the growth rate will change with the resolution. This is borne out to some extent. We have carried out global simulations with $0.1 < r/a < 0.9$ for plasma sizes of $a = 100\rho_u$ and $a = 200\rho_u$. With increased resolution in $y - z$ with $N_y = N_\parallel = 128$, but with reduced radial resolution, mode structures similar to Fig. 2 are obtained. It is mainly the global mode structure, which has small $k_\perp$, that requires the improved accuracy of the control-variate method in solving the Ampere's equation. Without the control-variate method, the global tearing eigenmode structure is not reproduced in simulations. The global simulations attempted here, though limited in scope, serve as an important verification of the algorithm for low-n tearing modes. The main challenge in applying full radius simulations to the linear $n = 1$ tearing mode in present tokamaks is not posed by getting the global mode structure accurate, but posed by the fine resolution near the resonance layer and the weak instability grow rate.

In the rest of the paper, we reduce the simulation domain to a narrow layer with $L_x/a \sim 0.01$, around the resonance surface at $r/a = 0.57735$ where $q = 2$. Here, L_x is the size of the simulated radial domain. On this short scale, the ion response is assumed to be adiabatic, $\delta n_i = -en_0\phi/T_i$. (Ion current response is neglected.) The boundary condition for $dA_\parallel(r)/dr$ at the inner and outer boundaries is taken from the eigenmode structure. We scan over a chosen parameter for the collisionless pure tearing mode, the semi-collisional pure tearing mode, and the collisionless drift-tearing mode, and compare simulation results with the analytical results, Eqs. (1), (3), and (5). To our knowledge, these analytic results have not been directly used to verify tearing mode simulations and verified with simulations. Previous GEM simulations of the collisionless and semi-collisional tearing modes are done in a slab geometry and verified directly with kinetic eigenmode results.[6]

A. Collisionless pure tearing mode

We first study the collisionless tearing mode by scanning over the electron mass and compare the simulation growth rate with Eq. (1). The electron mass enters the expression for γ_k through the electron thermal velocity v_e and the magnetic skin depth k_0^{-1}, such that $\gamma_k \sim \sqrt{m_e}$. The size of the plasma is

$a = 50\rho_u$, and the electron mass is scaled down to 16 times smaller than the physical value. Alternatively, one can choose a larger plasma size and scale up the electron mass. The radial domain is $L_x/a = 0.01$, centered at the $q = 2$ surface, with the boundary conditions $a_- = -0.408$ and $a_+ = -0.312$. Here, $a_- \equiv A'_\parallel/A_\parallel$ gives the radial slope of the vector potential at the inner boundary; a_+ is similarly defined. The values of a_+ and a_- at a fixed r/a scale inversely proportional to the plasma size. These boundary conditions are obtained from the reduced-MHD eigenmode structure. The number of grids is $(N_x, N_y, N_\parallel) = (512, 64, 64)$, and the number of particles is $8/cell$. Since ions are assumed to be adiabatic, the simulation is numerically stable without the split-weight scheme. As the electron mass is scaled down, the electron velocity is increased (the electron temperature is fixed), so the time step is also reduced. A time step of $\omega_u \Delta t = 0.5$ is used for the smallest m_e. The results are plotted in Fig. 3. Simulations with both the adiabatic ion response (green) and with ϕ set to zero (blue) are shown. The solid line shows the analytic results of Eq. (1) with $\Delta' a = 6$. All the analytic results are derived neglecting the effect of ϕ.[12]

The scaling of simulation results apparently approaches the analytical scaling as the electron mass decreases. The numerical values of simulations with $\phi = 0$ are also in reasonable agreement with the analytic results as m_e decreases. The deviation from the theoretical scaling at large electron mass can be attributed to the failure of the constant-Ψ approximation. Fig. 4 shows the mode structure from the simulation with the smallest electron mass of $m_p/m_e = 29392$. The collisionless tearing layer width is $\Delta_k \approx 0.0011\rho_u$, assuming $\Delta' a = 6$. The simulation domain is about $9\Delta_k$. The full layer width is to be understood as the layer width in which the mode structure deviates from the MHD mode structure. If we assume this layer width is about $5\Delta_k = 0.005\rho_u$ (see the ϕ mode structure of Fig. 4), then the value of $A_\parallel$ changes by about 10% over the layer width. At larger electron mass, the layer width is larger, and the constant-Ψ approximation will

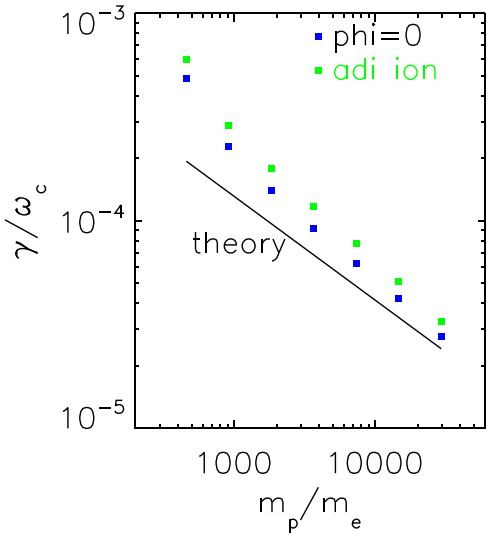

FIG. 3. Pure collisionless tearing mode growth rate vs. electron mass. Solid line from Eq. (1). Points are from simulation, green with adiabatic ions, blue with $\phi = 0$. As the electron mass becomes small, the growth rate approximately scales as $\gamma \sim m_e^{1/2}$.

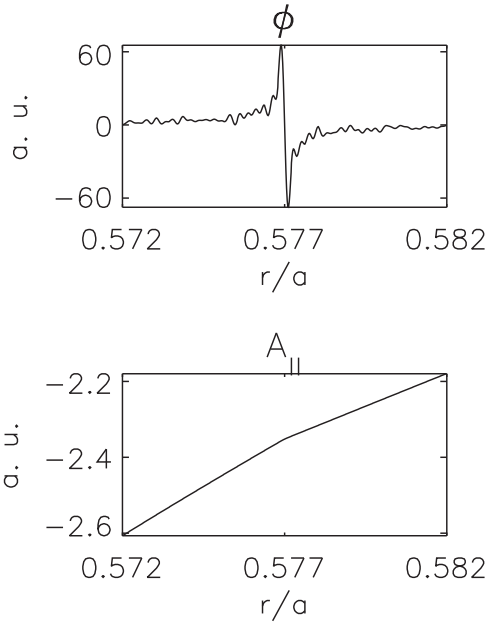

FIG. 4. Mode structure for the case of Fig. 3 with $m_p/m_e = 29392$ showing that $A_\parallel$ changes by about 10% across the tearing layer.

be violated by larger amounts. This explains the increasing deviation from the theoretical scaling at larger electron mass in Fig. 3.

B. Semi-collisional pure tearing mode

We now include an energy-dependent pitch-angle scattering collision operator in the electron kinetic equation. Collisions are implemented as scattering of the pitch-angle of the simulation particle and as a source term in the particle weight equation.[3] The random change to the pitch-angle during a time step is proportional to $\sqrt{\nu_c \Delta t}$. For accuracy, this random change must be much smaller than unity, which limits the time step at large collision rates. The collisional PIC algorithm is best suited for plasmas with weak collisions ($\nu_c/\omega_u \le 10^{-2}$), such as in the core of present day tokamaks. Drake and Lee[12] have shown that tearing modes in such plasmas are usually in the semi-collisional regime.

The semi-collisional scaling of Eq. (3) has not been observed in the previous gyrokinetic simulations.[10] Typically much weaker scaling such as $\gamma \sim \nu^{1/7}$ is observed. From the above collisionless simulations, we already see that the constant-Ψ approximation can be easily violated even in the collisionless regime. Collisions greatly broaden the tearing layer width and make it more difficult for this approximation to be valid. We have found it indeed very difficult to observe the $\gamma \sim \nu^{1/3}$ scaling. However, collisions are very important for tearing modes, and it is desirable to verify simulations with Eq. (3) for a case where the analytic result is expected. We therefore have carried out collision rate scan for equilibria with three different sizes, namely, $a = 100\rho_u$, $200\rho_u$, and $370\rho_u$. The grid resolution is $(N_x, N_y, N_\parallel) = (128, 64, 64)$, with 32 particles per cell. The size of the radial domain for the three plasma sizes is varied, roughly in accordance with the expected tearing layer width.

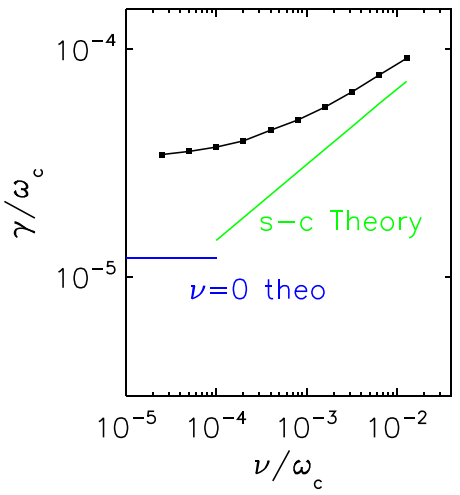

FIG. 5. Growth rate vs. collision rate for a plasma with $a = 100\rho_u$ showing the transition from the collisionless result (labeled "$\nu = 0$ theo") to the semi-collisional regime. The scaling with collision rate is weaker than the theoretical prediction with $\Delta' a = 6$ (green).

The results are shown in Figs. 5–7. For the small size case, Fig. 5, a smooth transition from the collisionless regime to the semi-collisional regime can be seen. Here "semi-collisional" is used in a loose sense, it refers to any scaling of the mode growth rate with the collision rate weaker than the classical resistive tearing mode scaling. The theoretical semi-collisional results, from Eq. (3), are shown in green line. One might suspect that the simulation results will approach theory if the collision rate is further increased, but this is not done, as the eigenmode structure (not shown) already indicates that the constant-Ψ approximation is broken for the high collision rates in Fig. 5. Because of this, it is impossible to estimate $\Delta' a$ from the simulation mode structure, and $\Delta' a = 6$ is used in the theoretical results of Fig. 5.

The collision rate scan for the case of $a = 200\rho_u$ in Fig. 6 is more clearly separated from the collisionless limit and shows an approximate power law scaling of $\gamma \sim \nu_c^{1/5}$, much weaker than the theoretical scaling of $\gamma \sim \nu_c^{1/3}$. Similar weak scaling has been reported in Eulerian simulations,[10] where

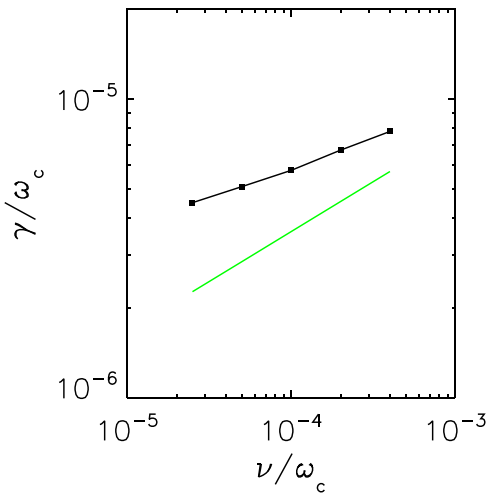

FIG. 6. Growth rate vs. collision rate for a plasma with $a = 200\rho_u$, green line from Eq. (3) with $\Delta' a = 6$.

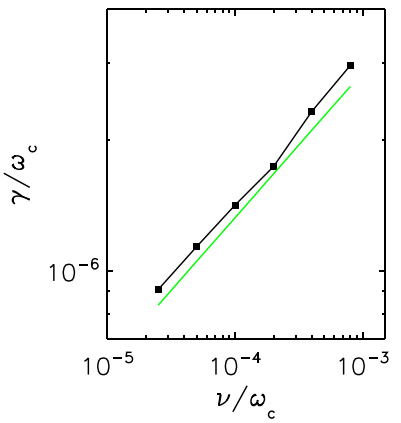

FIG. 7. Growth rate vs. collision rate for a plasma with $a = 370\rho_u$, showing agreement between simulation and theory with $\Delta' a = 8.5$ (green).

toroidal effects are included and the choice of the grid size is guided by the electron skin depth $\delta_e = c/\omega_{pe}$, much larger than Δ_k and Δ_{sc} for the present cases. Since the present plasma is strictly cylindrical, which is the same equilibrium used in the analytical study,[12] the disagreement with theory should not be overlooked. This consideration leads to the simulation of a plasma with $a = 370\rho_u$, roughly the size (in term of the minor radius) of DIII-D, as shown in Fig. 7. It should be noted that the simulation domain is very small for this case, $\Delta r/a = 0.0027$ or $\Delta r = \rho_u$. This is still larger than the semi-collisional layer width, Eq. (4), which gives $\Delta_{sc} = 0.75\rho_u$ for the largest collision rate in Fig. 7. Examination of the simulation mode structure indicates that $A_\parallel$ changes by less than 10% across the tearing layer for all the cases in Fig. 7. Simulation with such a small radial domain is possible only in linear simulations with cylindrical (or slab) geometry, where there is no particle radial motion. In toroidal geometry, a significant amount of the electrons will drift across the radial boundaries, and the simulation will be strongly affected by boundary effects. The analytic results of Fig. 7 are obtained with $\Delta' a = 8.5$ estimated from the simulation $A_\parallel$ mode structure. Fig. 7 shows good agreement between simulation and the analytical results in the scaling behavior, and the numerical values are also in reasonable agreement. This agreement provides an important verification of the collisional algorithm.

C. Collisionless drift-tearing mode

We now study the collisionless tearing mode with a finite electron temperature gradient. The starting case is the $m_p/m_e = 14\,696$ case of Fig. 3 for the small plasma size of $a = 50\rho_u$. The density profile is flat, but an electron temperature profile of the form

$$T_e(r) = T_0 \exp\left[-a\frac{\delta}{L_{Te}}\tanh\left(\frac{s - s_0}{\delta}\right)\right] \tag{7}$$

is used, with $s = r/a$, $s_0 = 0.57735$ at the $q = 2$ surface, $\delta = 0.5$, and L_{Te} is the temperature scale length. With the small simulation domain, this temperature profile yields nearly a constant temperature and constant gradient in the simulation domain. We vary the temperature scale length and compare

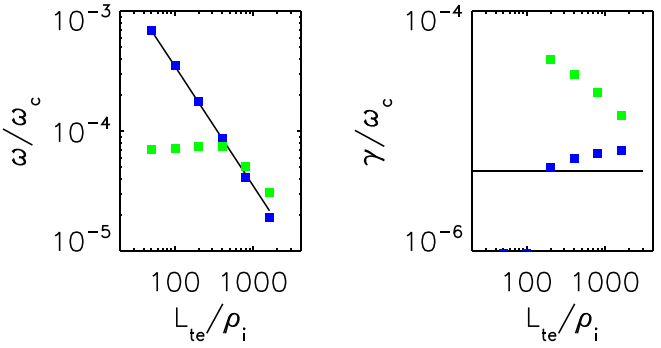

FIG. 8. Drift-tearing mode frequency (left) and growth rate (right) from simulation (points) and theory (solid line). Blue points are with $\phi = 0$, green points with adiabatic ions. The mode frequency with $\phi = 0$ agrees with theory, Eq. (5).

the simulation frequency and growth rate with theory. The results are shown in Fig. 8. The simulation mode frequency with $\phi = 0$ (blue points) agrees well with Eq. (5) (solid line). The mode growth rate is insensitive to the temperature gradient for weak gradient values and approaches the pure tearing mode growth rate (corresponding to $L_{\mathrm{Te}} = \infty$). This is also in agreement with theory. The stabilization of the mode at lower L_{Te} values is again caused by the failure of the constant-Ψ approximation; as according to Eq. (6), the tearing layer width of the drift tearing mode is proportional to $\omega_T^* \propto 1/L_{\mathrm{Te}}$. The simulation results with adiabatic ions (green points) deviate from the results with $\phi = 0$ more drastically with a finite temperature gradient. Compared with Fig. 3, the destabilization effect of ions is more pronounced as the temperature gradient increases. Moreover, the mode frequency becomes much smaller and independent of the temperature gradient for small L_{Te} values. These observations suggest strong interaction between the drift effect and the electrostatic potential.

We can summarize the simulation/theory comparison. The theoretical analysis is based on the constant-Ψ approximation. In general, weaker instability (narrower tearing layer width) leads to better validity of this approximation. When this approximation is valid, the main analytic results are all verified.

IV. SUMMARY

The main purpose of this paper is verification. Direct simulation of low-n tearing modes with fully kinetic electrons is carried out for the first time with the particle-in-cell δf-method. Problems in various limits, such as strict cylindrical geometry, a thin radial domain, small electron mass, and adiabatic ion responses, are used, so that the simulation results can be directly compared with the analytic theory. The constant-Ψ approximation is heavily used in theoretical studies. We have shown that, in cases of weak instabilities where this approximation is valid, simulation results agree with the theoretical predictions. The growth rate of the collisionless tearing mode scales with the electron mass as $\gamma \sim \sqrt{m_e}$; in the semi-collisional regime, the growth rate scales with the electron collision rate as $\gamma \sim \nu_c^{1/3}$; and in the collisionless drift tearing mode, frequency is proportional to the drift frequency ω^*, with the growth rate insensitive to ω^* for weak instabilities. All these are in agreement with the theory. The global mode structure also agrees very well with MHD eigenmode calculations, even if the tearing layer is not sufficiently resolved. The experience gained from this study will be a guide to future toroidal nonlinear simulations, in choosing simulation parameters such as grid resolution, time step, and the number of particles. Some conclusions can be drawn based on the present study. It is impractical to carry out radially global simulations of the collisionless tearing modes due to the large number of radial grid points (assuming uniformly spaced), similarly for the pure tearing mode in the semi-collisional regime with low collisionality. One way to alleviate the problem is to use a reduced radial domain, as in most of the simulations in this paper. The boundary conditions on the reduced domain are obtained from the external solution that can be computed with fluid models. This method is useful for the linear stage and the early nonlinear stage where the island width is small. A natural solution to the resolution problem is to use nonuniform radial grids, i.e., use fine grids only near the tearing layer. We will explore this approach in the future.

ACKNOWLEDGMENTS

This work was supported by the U.S. Department of Energy's SciDAC projects "Center for Nonlinear Simulation of Energetic Particles in Burning Plasmas" (DE-FG02-08ER54987), "Center for Edge Physics Simulation" (DE-SC0008801), and "Center for Extended Magnetohydrodynamic Modeling" (DE-FC02-08ER54971). This research used resources of the National Energy Research Scientific Computing Center, which is supported by the Office of Science of the U.S. Department of Energy under Contract No. DE-AC02-05CH11231.

[1]B. C. Lyons, S. C. Jardin, and J. J. Ramos, Phys. Plasmas **22**, 056103 (2015).
[2]Y. Chen, J. Chowdhury, S. E. Parker, and W. Wan, Phys. Plasmas **22**, 042111 (2015).
[3]Y. Chen and S. E. Parker, J. Comput. Phys. **189**, 463 (2003).
[4]Y. Chen and S. E. Parker, J. Comput. Phys. **220**, 839 (2007).
[5]R. D. Sydora, Phys. Plasmas **8**, 1929 (2001).
[6]W. Wan, Y. Chen, and S. Parker, Phys. Plasmas **12**, 012311 (2005).
[7]B. N. Rogers, S. Kobayashi, P. Ricci, W. Dorland, J. F. Drake, and T. Tatsuno, Phys. Plasmas **14**, 092110 (2007).
[8]R. Numata, W. Dorland, G. G. Howes, N. F. Loureiro, B. N. Rogers, and T. Tatsuno, Phys. Plasmas **18**, 112106 (2011).
[9]H. Doerk, F. Jenko, M. J. Pueshel, and D. R. Hatch, Phys. Rev. Lett. **106**, 155003 (2011).
[10]W. A. Hornsby, P. Migliano, R. Buchholz, L. Kroenert, A. Weikl, A. G. Peeters, D. Zarzoso, E. Poli, and F. J. Casson, Phys. Plasmas **22**, 022118 (2015).
[11]J. Chowdhury, Y. Chen, W. Wan, S. E. Parker, W. Guttenfelder, and J. M. Canik, "Particle-in-cell delta-f gyrokinetic simulations of the microtearing mode," Phys. Plasmas (to be published).
[12]J. F. Drake and Y. C. Lee, Phys. Fluids **20**, 1341 (1977).
[13]H. P. Furth, J. Killeen, and M. N. Rosenbluth, Phys. Fluids **6**, 459 (1963).
[14]R. Hatzky, A. Konies, and A. Mishchenko, J. Comput. Phys. **225**, 568 (2007).
[15]A. Mishchenko, A. Konies, R. Kleiber, and M. Cole, Phys. Plasmas **21**, 092110 (2014).
[16]Y. Chen, S. E. Parker, W. Wan, and R. Bravenec, Phys. Plasmas **20**, 092511 (2013).
[17]J. L. Luxon and L. G. Davis, Fusion Technology **8**, 441 (1985).
[18]Y. Chen and S. E. Parker, Phys. Plasmas **18**, 055703 (2011).
[19]E. A. Startsev and W. W. Lee, Phys. Plasmas **21**, 022505 (2014).